J. Fluid Mech. (1983), *vol.* 131, *pp.* 271–287
Printed in Great Britain

A liquid compound jet

By C. H. HERTZ AND B. HERMANRUD†
Department of Electrical Measurements, Lund Institute of Technology, S-220 07 Lund, Sweden

(Received 9 November 1982)

The principle and basic physics of a new type of liquid-in-air jet are described. This jet is generated by a primary fluid jet that emerges from a nozzle below the surface of a stationary (secondary) fluid. After breaking the surface, the jet consists of the central primary jet surrounded by a sheath of secondary fluid which has been entrained by the primary jet during its passage through the secondary fluid. Normally the flow in this compound jet is laminar, and it breaks up into drops due to capillary instability.

In this paper the generation of compound jets is discussed, and the flow pattern in the jet is studied experimentally both in stable and unstable conditions. Three different types of instabilities can be elicited on the jet. The jet mechanism is described quantitatively, and expressions for the jet velocity and some other parameters are derived.

1. Introduction

During the last decade, fluid jets in air have been studied intensely because of their applications in ink-jet printing (Sweet 1964; Hertz & Månsson 1972; Kamphoefner 1972) and particle sorting (Herzberg, Sweet & Herzberg 1976). In these applications, jets of small diameter (10–60 μm) and high velocity (10–40 m/s) are produced by forcing a low-viscosity fluid (1–5 cP) under high pressure through a nozzle into air. Shortly after leaving the nozzle the jet disintegrates into a train of drops owing to axisymmetric capillary instabilities first studied by Rayleigh (1879). It was shown by Sweet (1964) that these drops could be electrically charged by a signal voltage and subsequently deflected in a transverse electric field. This method to control the direction of the jet by a signal voltage is used in ink-jet printing and particle sorting.

Because of the small nozzle diameters used in these applications, the choice of inks is very limited (Ashley, Edds & Elbert 1977). Among other restrictions it might be mentioned that the use of pigmented inks is impossible because of nozzle or filter clogging by pigment particles.

To avoid these difficulties, a new method to generate a fluid jet in air from an orifice much larger than the jet diameter has been developed (Hermanrud & Hertz 1979). The fluid flow and instabilities of this new type of jet differ from those of ordinary fluid jets in air. It is the purpose of this paper to describe the jet generation principle as well as to give a qualitative description of the hydrodynamics of the jet.

2. Principle of the compound jet

While conventional fluid jets normally issue from a nozzle, the new type of jet emerges from the surface of an essentially stationary fluid. Figure 1 shows the

† Present address: Siemens–Elema AB, Solna, Sweden.

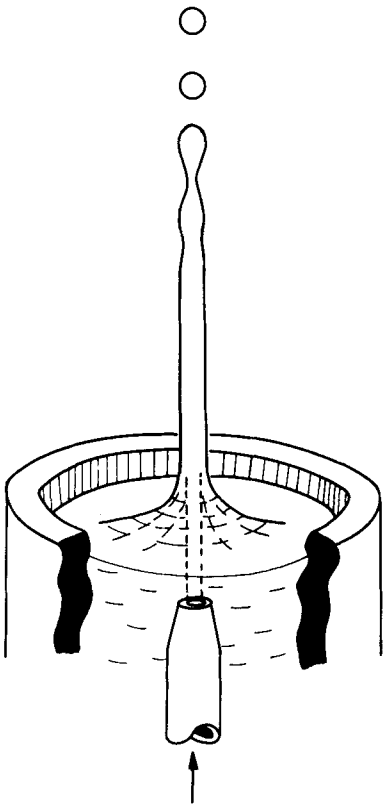

FIGURE 1. Generation of a compound jet. A high-speed liquid jet emerges from a nozzle a short distance below the surface of a stationary fluid. After breaking the surface, the primary jet carries a concentric layer of the stationary (secondary) fluid, which, owing to viscous forces, has been entrained by the primary jet during its passage through the secondary fluid.

arrangement used to generate such a jet. Here a nozzle is submerged below the surface of the stationary fluid. Through this nozzle a suitable 'primary' fluid is forced under high pressure. In this way a liquid-in-liquid jet is generated in the stationary fluid, which in the following will be called 'secondary' fluid. In passing through the stationary (secondary) fluid the primary jet causes adjoining secondary fluid layers to be accelerated through viscous forces. Thus, when emerging into air the jet consists of a cylindrical core of primary jet fluid surrounded by a concentric layer of secondary fluid travelling at nearly the same speed. The jet emerging from the surface will therefore be called a *compound jet* in the following. The amount of secondary fluid entrained by the primary jet depends, among other parameters, on the distance from the nozzle to the surface of the secondary fluid. Compound jets in air spontaneously break up into drops owing to axisymmetric capillary instabilities in the same way as conventional jets (Rayleigh 1879).

Stable compound jets have been demonstrated in our laboratory with diameters from 15 μm to 1 mm, but most of the work reported here has been performed with 75 μm jets with jet velocities around 10 m/s. While the secondary-fluid surface from which the compound jet emerges can in principle be of any size, normally it is contained in tubes having diameters of 1–2 mm as shown in figure 1. This has the advantage that the orifice from which the compound jet issues can be placed in any position, since surface tension prevents secondary fluid from flowing out of the orifice

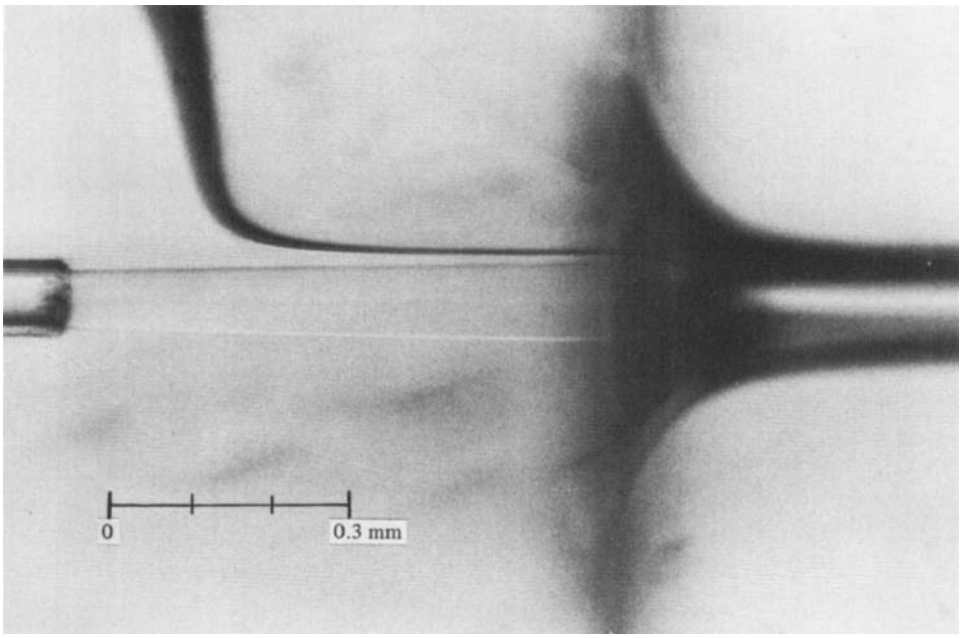

FIGURE 2. Microphotograph of compound-jet generation. A primary jet (20 % ethanol + 80 % water) emerges from a 75 μm nozzle to the left into pure water and emerges through the water surface into air, thereby forming a compound jet (right). Coloured tracer fluid added at the top of the figure (black trace) indicates a streamline in the water. $\bar{v}_{p0} = 11.5$ m/s, primary-jet flow 51 μl/s, secondary-fluid flow 72 μl/s. Distance from nozzle to point of drop formation 20 mm.

owing to gravity. On the other hand, such an orifice is large enough to allow the passage of small particles or pigments in the secondary fluid or to alleviate the problem of drying. For convenience horizontal jets were normally used.

Figure 2 shows a microphotograph of a typical stable compound jet used in our studies. A primary jet consisting of an ethanol–water mixture issues from a 75 μm glass tube at a speed of 11.5 m/s into a secondary fluid of pure water. After travelling for approximately 0.75 mm, the jet breaks the surface of the secondary fluid and emerges into air. The slight divergence of the jet indicates that the primary jet is heavily decelerated by viscous drag, its momentum diffusing radially into the secondary fluid. The resulting acceleration of second fluid layers close to the primary jet is shown by the line of coloured tracer fluid which was added slowly to the secondary fluid from a small nozzle placed outside the top of figure 2. Finally, the jet emerging into air on the right side of figure 2 consists of both primary and secondary fluid, as indicated by its large diameter of about 150 μm. Thus it is a compound jet.

In a compound jet, secondary fluid is continuously carried away by the primary jet. Therefore, if the compound-jet parameters are to be kept constant, secondary fluid has to be supplied continuously to the system. In the present investigation this was achieved by a peristaltic pump. Since under stationary conditions all secondary fluid supplied to the nozzle is carried away by the primary jet, control of secondary-fluid flow by regulating the speed of the pump essentially determines the diameter, composition and velocity of the compound jet.

It will be shown below that the accelerations encountered close to the boundary between the primary jet and the secondary fluid are quite large. Also the first

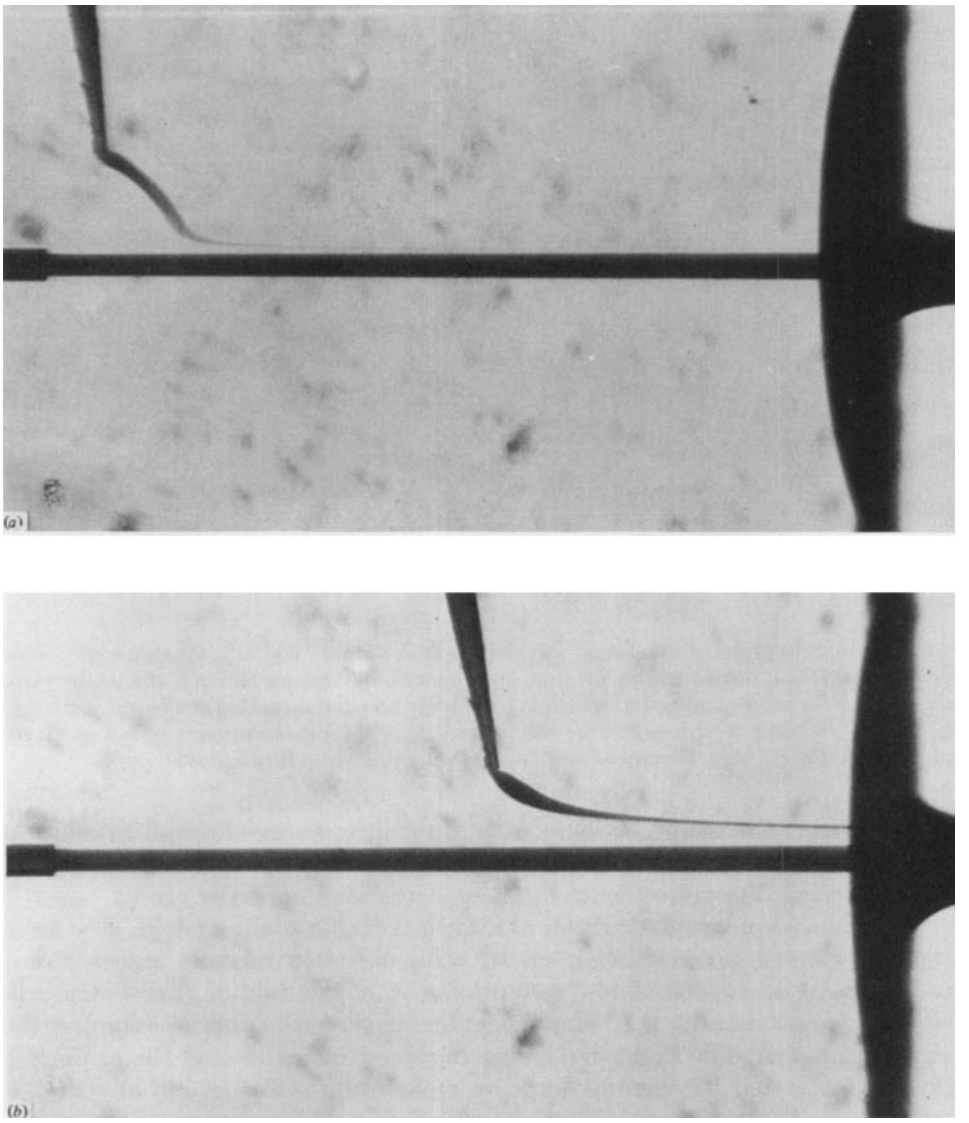

FIGURE 3(*a*, *b*). For caption see facing page.

derivative of the velocity is discontinuous at this boundary. Therefore it is to be expected that instabilities are easily formed which propagate and grow in the jet direction. Three types of instabilities have been observed and will be discussed below.

3. Fluid dynamics of stable jets

In most of the experiments of the present investigation the secondary fluid was contained in an elongated rectangular vessel 2×2 mm^2 in cross-section instead of the tube shown in figure 1 (Hermanrud 1981). A glass tube (outside diameter 100 μm, inside diameter 75 μm) was inserted halfway into the vessel along its long axis, the opposite side being open to allow for the exit of the compound jet. Two opposite walls of the vessel were formed by microscope coverslips which made it possible to observe

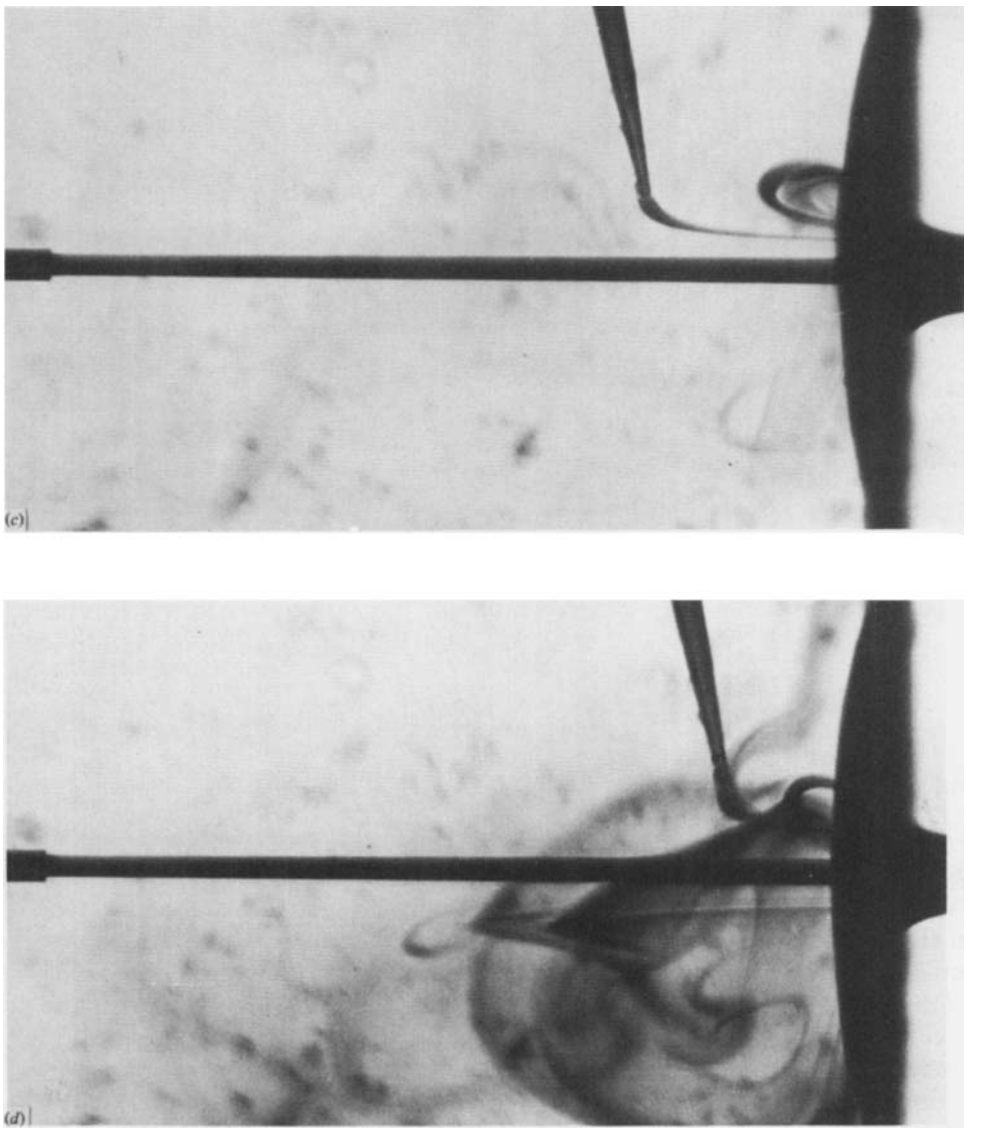

FIGURE 3. Streamlines in the secondary fluid shown by a coloured tracer which issues from a fine glass nozzle above the primary jet. Accelerated but laminar flow is indicated for secondary fluid layers close to primary jet (*a*, *b*). Eddies develop at secondary-fluid surface (*c*, *d*). Primary-jet diameter 75 μm, $\bar{v}_{p0} = 8.1$ m/s, $\eta_p = 1.9$ cP, viscosity of secondary fluid $\eta_s = 1.7$ cP, $Re_p = 320$.

the interior of the vessel with a microscope. To observe the streamlines in the secondary fluid a coloured tracer fluid was added very slowly from a 15 μm nozzle which could be moved parallel to the jet direction (figures 2 and 3).

3.1. *Generation of the compound jet*

In figure 3 the nozzle introducing the tracer fluid was moved parallel to the jet direction to show different streamlines. The photographs indicate that the streamlines close to the nozzle roughly follow the pattern predicted by Landau & Lifshitz (1959) for an infinitesimal jet in an unbounded outer fluid. However, since the diameter of the primary jet cannot be neglected in comparison with the size of the chamber

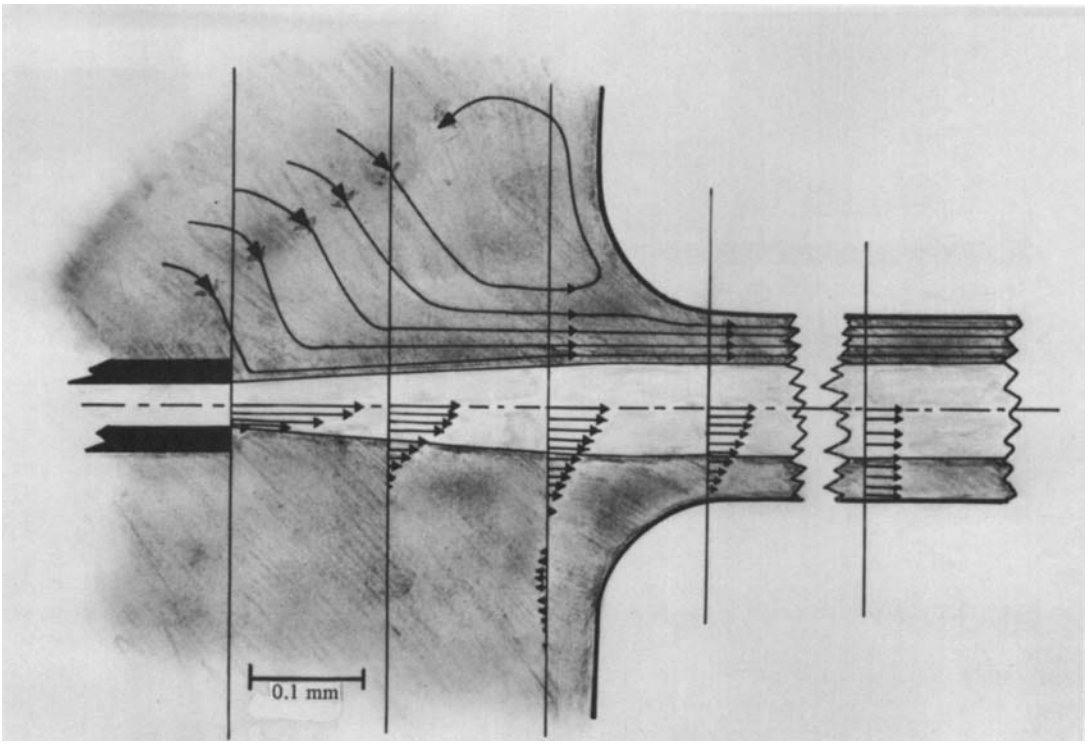

FIGURE 4. Qualitative picture of streamlines in compound jet arrangement shown in figure 3. Upper half of the picture: streamlines, lower half: axial velocity component.

containing the secondary fluid, no quantitative comparison could be made. Further, the viscosities of the two liquids used in figure 3 were not the same.

In the immediate vicinity of the secondary-fluid surface, eddies can be observed (figures 3*c*, *d*). They are due to the fact that fluid layers situated relatively far away from the jet axis cannot enter the compound jet funnel and are reflected at the fluid surface. Observation of the tracer fluid indicates that this fluid returns towards the primary jet in an irregular manner.

Figure 3 indicates that the primary jet does not mix with secondary fluid before emerging into air. For jet parameters used here its flow is essentially laminar. Such jets can be generated independently of the velocity profile of the primary jet at the nozzle exit.

On its way through the secondary fluid, the primary jet loses speed owing to diffusion of momentum into the secondary fluid. This results in an increase of jet diameter as shown in figures 2 and 3.

From tracer experiments we obtain the qualitative picture of streamlines that is given in figure 4. Since the primary jet exits from a 2 cm long glass tube its velocity profile near the nozzle is parabolic (Langhaar 1942). Then, on its way to the secondary-fluid surface the primary jet, as we have seen, loses momentum to the secondary fluid. However, using the results obtained by Schlichting (1933) and Andrade & Tsien (1937) it can be estimated that more than 99 % of the momentum originally supplied to the primary jet enters the compound-jet funnel in most cases. Less than 1 % of the momentum is reflected at the secondary-fluid surface, giving rise to the eddies of figures 3(*c*, *d*).

We are not aware of any analytical solution of the flow in a liquid-into-liquid jet in the literature apart from the idealizations of Landau & Lifshitz (1959) and Schlichting (1933). A quantitative comparison of the flowlines observed in figure 3 with theory was therefore not possible. The stability of liquid-into-liquid jets has been investigated both theoretically (Batchelor & Gill 1962; Lessen & Singh 1973) and experimentally (Andrade & Tsien 1937; Reynolds 1962; McNaughton & Sinclair 1966). However, in most of these papers the density and viscosity of the two liquids involved were the same, and so even these results could not be applied to the present investigation.

If the viscosities η_p and η_s of the primary and secondary fluids are different, we have to distinguish between two different velocity profiles of the liquid-in-liquid jet. Since the shear forces and the velocity in the fluids are continuous at the boundary between the primary jet and the secondary fluid, we find

$$\eta_p\left(\frac{\delta v_p(r)}{\delta r}\right)_{R_p} = \eta_s\left(\frac{\delta v_s(r)}{\delta r}\right)_{R_p}, \tag{1}$$

where $v_p(r)$ and $v_s(r)$ are the velocities in the jet direction of the primary and secondary fluids respectively and $R_p(x)$ is the radius of the primary jet.

Thus if $\eta_p \neq \eta_s$ there is a discontinuity in the derivative of the axial velocity $v(r)$ at this boundary which might cause instabilities. The equation suggests that such instabilities should develop more easily if $\eta_p < \eta_s$ than if $\eta_p > \eta_s$. This is substantiated by experimental evidence.

3.2. *Compound jet in air*

After breaking the surface of the secondary fluid, the primary jet emerges into air surrounded by a sheath of secondary fluid, thus forming a compound jet. In the following, some experimental and theoretical results concerning the properties of a laminar-flow compound jet will be presented.

Figure 5 shows different parts of a compound jet generated by a 75 μm coloured primary jet in a clear secondary fluid. The physical properties of both fluids are equal. The distance between the base of the compound jet and the point of drop formation was 22 mm. The microphotograph shows clearly that the jet consists of a central primary-fluid column, which is surrounded by a coaxial sheath of secondary fluid. No visible mixing due to flow instabilities or molecular diffusion occurs between the two fluids before the jet disintegrates into drops at the point of drop formation. Even after drop formation the boundary between primary and secondary fluid is well defined in each drop, although it becomes irregular.

From the micrographs in figure 5, as well as the fact that the capillary instability causing drop formation is quite symmetric, it can be concluded that the flow in the jet is essentially laminar. Thus the primary and secondary fluids can mix only by molecular diffusion across the boundary between the two liquids. The diffusion length r_d can be estimated from the expression (Einstein 1907)

$$r_d = (2Dt)^{\frac{1}{2}}, \tag{2}$$

where t is the time of flight of the primary jet from the nozzle to the point of drop formation and D is the constant of diffusion. Since for fluids D is of the order of 10^{-5} cm^2/s and t about 3 ms in the present case, we find $r_d = 2.5$ μm. Thus we cannot expect to observe the mixing due to molecular diffusion in the photographs of figure 5. For all practical purposes this effect can be neglected.

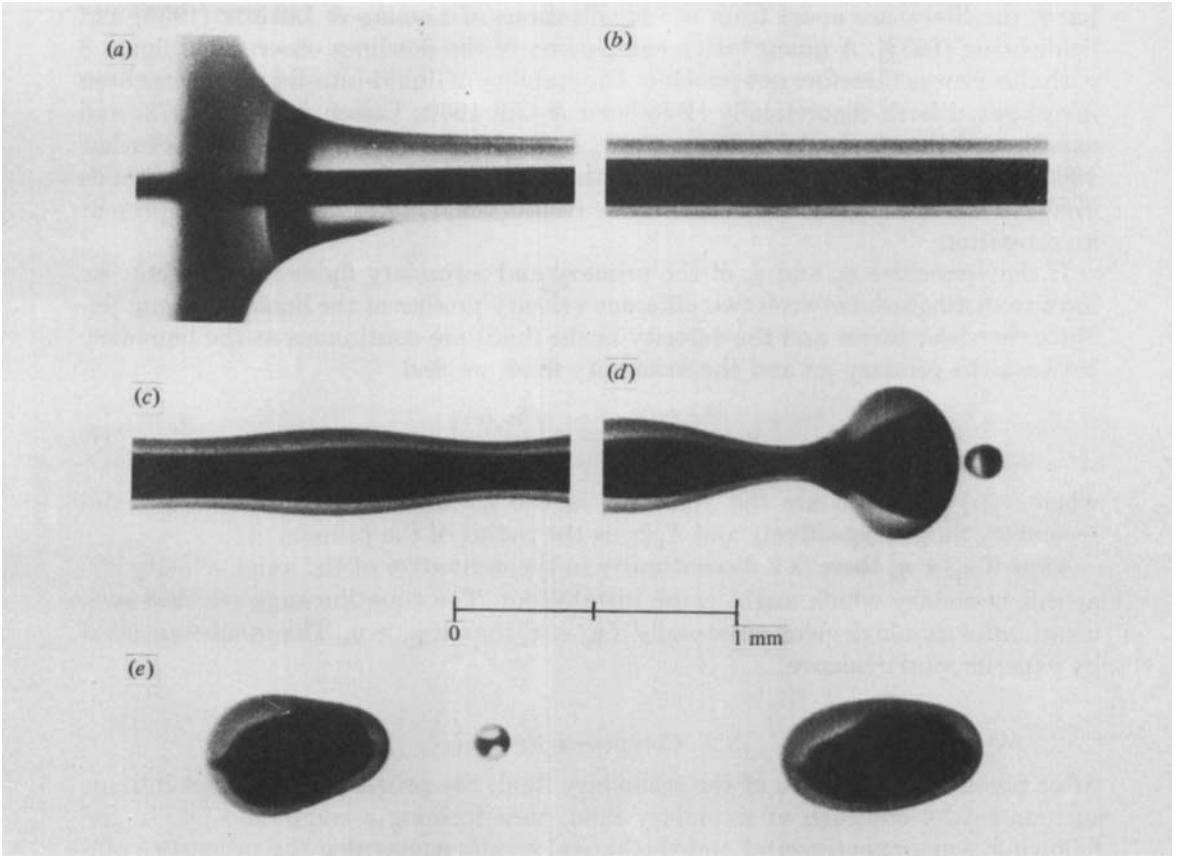

FIGURE 5. Compound jet in air. Actual distance from secondary-fluid surface to point of drop formation 22 mm, primary-jet diameter 75 μm, velocity $\bar{v}_{p0} = 8.1$ m/s. Five segments of the jet are shown: (*a*) compound jet base; (*b*) 10 mm from base; (*c*) 3 mm from point of drop formation; (*d*) point of drop formation; (*e*) 3 mm after point of drop formation. Primary fluid 80 % H_2O + 20 % glycerol and dye, flow 36 μl/s, secondary fluid 80 % H_2O + 20 % glycerol without dye, flow 115 μl/s, $v_c = 2.6$ m/s. Owing to refraction of light in the secondary fluid, the diameter of the primary-fluid column is enlarged in the picture. Exposure time 3 μs.

Hermanrud (1981) has investigated the surface flow close to the jet funnel (cf. figure 5*a*) and demonstrated a stagnation point about one jet diameter from the jet axis. This corresponds to the eddy shown in figure 3(*c*).

3.3. *Momentum flux in the compound jet*

It has been mentioned earlier that in most cases more than 99 % of the primary-jet momentum is carried away by the compound jet. Since the secondary fluid is initially almost at rest, the momentum flux in the compound jet is practically equal to the momentum flux in the primary jet when emerging from the nozzle. Therefore some of the compound-jet parameters can be calculated.

Let Q_p be the flow or volume flux of the primary jet emerging with an average speed $\bar{v}_{p0}$ from a nozzle with a diameter $2R_{p0}$. By definition $\bar{v}_{p0} = Q_p/\pi R_{p0}^2$. Since the nozzle is a glass tube the length of which is more than 200 times its diameter, the jet has a parabolic velocity profile when leaving the nozzle (Langhaar 1942). The maximum

speed in the jet is then $\hat{v}_{p0} = 2\bar{v}_{p0}$. For the momentum flux M_p of the primary jet we have (Batchelor & Gill 1962)

$$M_p = \frac{4}{3}\frac{\rho_0 Q_p^2}{\pi R_{p0}^2}. \tag{3}$$

Now, the coaxial geometry of the compound jet allows us to calculate its momentum flux M_c. If ρ_p and ρ_s are the densities and R_p and R_c the radii of the primary fluid column and the secondary-fluid sheath, we find

$$M_c = 2\pi \int_0^{R_p} \rho_p v(r)^2 r\,dr + 2\pi \int_{R_p}^{R_c} \rho_s v(r)^2 r\,dr, \tag{4}$$

where the first term is the momentum flux of the primary-fluid column and the second that of the secondary-fluid sheath. The unknown function $v(r, x)$ represents the velocity component parallel to the jet axis x. The radii R_p and R_c are also functions of x.

However, shortly after entering the compound-jet funnel the velocity distribution in the jet assumes a plug-flow profile with $v(r, x) = v_c$, $R_p = R_{p\infty}$, $R_c = R_{c\infty}$ (constant). The length for this transition can be estimated by using a relation given by Brun & Lienhard (1968), who showed that the length l of the velocity-profile relaxation in a conventional jet from parabolic to plug-flow profile is given by

$$l = 0.05\, Re\, R, \tag{5}$$

where R and Re are respectively the radius and Reynolds number of the jet. In our application of (5) we have to choose R somewhat larger than R_{p0}. For the jet shown in figure 2, $R_{p0} = 37.5$ μm and $Re = 242$, we find $l = 0.8$ mm or a little more, but much shorter than the break-up length due to capillary instabilities of the compound jet (22 mm). This fact can also be deduced from the microphotographs, since the diameter of the compound jet does not change after having travelled in air for about 1 mm.

Thus, shortly after emerging from the secondary fluid, the compound jet assumes a plug-flow profile, i.e. $v(r, x) = v_c$ = constant. For plug flow the integrals in (4) are elementary. Using the relation

$$Q_c = Q_p + Q_s = \pi R_c^2 v_c, \tag{6}$$

where Q_c, Q_p and Q_s are the flows of the compound jet and the primary and secondary fluids, we find for the momentum flux M_c of the compound jet

$$M_c = \frac{Q_c}{\pi R_c^2}(\rho_p Q_p + \rho_s Q_s). \tag{7}$$

It should be observed that surface tension causes an axial pressure gradient at the compound jet base. However, in normal jets this gradient is only of the order of a few percent of the gradient caused by deceleration, and is therefore disregarded here. Then, from (3) and (7) and the fact that the momentum flux M_c is nearly equal to the momentum flux M_p in the primary jet, we find for the velocity v_c of the compound jet

$$v_c \leqslant \frac{\rho_p Q_p}{\rho_p Q_p + \rho_s Q_s} v_p, \tag{8}$$

where $v_p = \frac{4}{3}\bar{v}_{p0}$ is the plug-flow speed of the primary jet in air, without a secondary fluid. From (8) we get a quantitative expression of the fact, already noted, that the

secondary fluid is accelerated and the primary jet decelerated during the generation of the compound jet.

Further, since $$Q_p = \pi R_{p0}^2 \bar{v}_{p0} = \pi R_{p\infty}^2 v_c,$$

we find from (8) $$R_{p\infty} \geqslant \left[\frac{3}{4}\frac{\rho_p Q_p + \rho_s Q_s}{\rho_p Q_p}\right]^{\frac{1}{2}} R_{p0}, \tag{9}$$

i.e. the radius $R_{p\infty}$ of the primary fluid in the compound jet is larger than the plug-flow radius $(\frac{3}{4}R_{p0})^{\frac{1}{2}}$ of the primary jet in air.

3.4. *Acceleration in the compound jet*

We shall now try to calculate the accelerations that occur in the primary and secondary fluid during the formation of the compound jet. Since the flowline distribution for the fluid-in-fluid jet is not known, only the order of magnitude of the acceleration can be estimated.

The maximum speed of the primary jet $\hat{v}_{p0} = 2\bar{v}_{p0}$ in the centre of the nozzle decreases to v_c when the primary jet has entered the compound jet and plug-flow distribution is attained. Thus we find for the average deceleration

$$a = \frac{\hat{v}_{p0}^2 - v_c^2}{2s}. \tag{10}$$

The distance from the nozzle to the point of plug flow in the compound jet must somewhat exceed the relaxation length l of (5). Using $s = 1$ mm and (8) and (10) we find for the average deceleration along the axis of the jet shown in figure 2, $a = 1.37 \times 10^7$ cm/s^2, or approximately $14000g$.

Since the secondary fluid starts essentially from rest, we find for the average acceleration of the secondary fluid layers at the boundary of the primary jet

$$a = \frac{v_c^2}{2s} \tag{11}$$

For the jet in figure 2 this gives $a = 1.1 \times 10^6$ cm/s$^2 \approx 1200g$.

Obviously the acceleration is not uniform along the jet axis as assumed above. Therefore the maximum acceleration occurring during the generation of the compound jet shown in figure 2 must be appreciably higher. Using primary jets having a diameter of 10 μm and a velocity of 40 m/s, average accelerations as high as 10^4–$10^5 g$ have been observed in laminar and stable compound jets. It is obvious that these large accelerations correspond to large shear forces in the fluids. Therefore instabilities are easily generated as shown below.

3.5. *Reynolds number of the compound jet*

If the dynamic viscosities of the primary and secondary fluids are not too different, it is reasonable to define a Reynolds number for the compound jet as

$$Re_c = \frac{2v_c R_c}{\nu}, \tag{12}$$

where the value of ν lies somewhere between the values of the dynamic viscosities of the primary and secondary fluid.

Let us assume that the viscosities and densities of the primary and secondary fluids

are very similar, i.e. $\eta_p \approx \eta_s \approx \eta$ and $\rho_p \approx \rho_s \approx \rho$. Then we find for the momentum flux of the compound jet (7)

$$M_c = \frac{\rho Q_c^2}{\pi R_c^2} = \pi R_c^2 v_c^2. \tag{7'}$$

Thus we can write for the Reynolds number

$$Re_c = \frac{2}{\nu}\left(\frac{M_c}{\rho\pi}\right)^{\frac{1}{2}}. \tag{13}$$

By the same reasoning we find the Reynolds number of the primary jet (cf. (3))

$$Re_p = \frac{2\bar{v}_p R_p}{\nu_p} = \frac{2}{\nu_p}\left(\frac{M_p}{\rho_p \pi}\right)^{\frac{1}{2}}. \tag{14}$$

Comparing (13) and (14), we find

$$Re_c \approx Re_p, \tag{15}$$

under the assumption that $\rho_p \approx \rho_c$ and $\eta_p \approx \eta_s$.

4. Compound-jet instabilities

Except for the capillary instability leading to drop formation observed in conventional fluid jets (Rayleigh 1879; Chaudhary & Redekopp 1980), two other types of instabilities can be demonstrated in the compound jet. These latter instabilities are due to large internal shear forces as well as to the velocity distribution in the fluids.

Since all instabilities observed are initiated by small disturbances, their respective speed of growth determines which of the three instabilities develops fastest and therefore visibly dominates the jet. This speed of growth depends on the jet parameters. Large velocities or high flow rates seem to favour the non-capillary types of instabilities, but they depend also on the viscosity of the primary and secondary fluids. In the following, examples of these instabilities will be given.

4.1. *Capillary instability*

Rayleigh (1879) investigated the instability due to capillary forces which eventually leads to the disintegration of the jet into drops. The theory was improved by Weber (1931) by including the viscosity of the fluid into the calculations. Recently, Chaudhary & Redekopp (1980) were able to explain the formation of so-called satellite drops between the main drops in the jet break-up process.

As shown in figure 5, the drop formation in the compound jet due to capillary instability is the same as in the conventional jet. This is to be expected for the jet in figure 5, where the parameters of the primary and secondary fluid were essentially equal, but is also true for jets formed from fluids showing differences in viscosity and surface tension as large as 1:3 or 1:4. In the jet shown in figure 5 the ratio of primary to secondary fluid flow was adjusted to 1:3.2 by controlling the secondary-fluid flow supplied by the peristaltic pump. This unusually large flow ratio was chosen to facilitate the visualization of the primary fluid column in the compound jet. The column is otherwise hard to see because of light refraction in the cylindrical surface of the jet, which enlarges the apparent diameter $2R_a$ of the primary fluid. From optical considerations one finds that $R_a = nR_{p\infty}$ (Hermanrud 1981), where $R_{p\infty}$ is its actual radius and n the index of refraction of the secondary fluid ($n = 1.33$). Thus the actual diameters of the compound jet and the primary fluid column are 270 μm and 133 μm respectively. The optical distortion of the shape of the primary fluid is

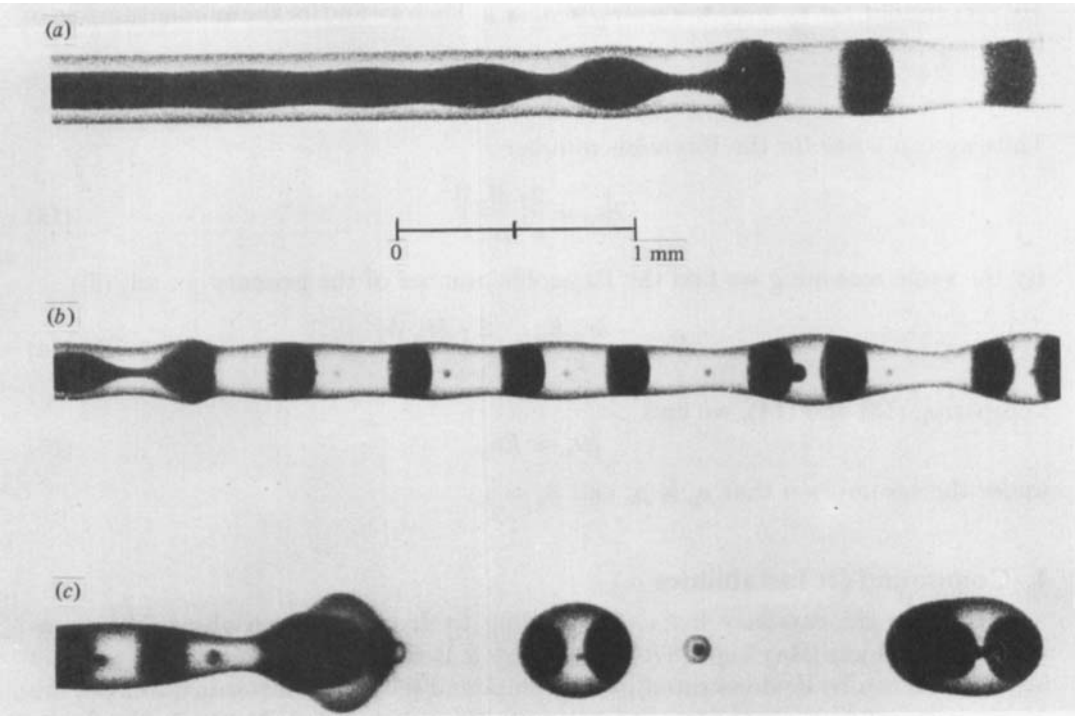

FIGURE 6. Drop-formation points of compound jet formed by a primary jet of 80% H_2O + 20% glycerol + dye with silicon fluid as secondary fluid. Surface tension of primary fluid 72 dyn/cm, that of secondary fluid 20 dyn/cm. Surface tension at interface primary–secondary fluid about 52 dyn/cm. This causes drop formation of primary-fluid column (*a*, *b*) much earlier than drop formation of compound jet (*c*). Viscosity in primary and secondary fluid about the same (2 cP), $\bar{v}_{p0} = 8.1$ m/s, $Q_p = 36$ µl/s, $Q_s = 115$ µl/s. Distance from nozzle to final point of drop formation about 25 mm.

even more pronounced at the base of the compound jet and in the drops, since the secondary-fluid surface has a double curvature in these cases.

In figure 5 no instabilities other than the capillary instability leading to drop formation can be detected on the primary-fluid column. Even during drop formation no mixing of secondary and primary fluid occurs, as indicated by the well-defined boundary between primary and secondary fluids in the drops. Thus, in this case, capillary instabilities causing normal drop formation dominate over the instabilities described below. Satellites are formed as in conventional jets. However, satellite formation is influenced by the choice of primary- and secondary-fluid viscosity.

Laminar-flow jets as shown in figure 5 can be produced readily with a large range of fluid parameters. We have successfully used primary jet diameters in the range 0.01–1 mm, primary-jet speeds from 5 to 40 m/s, primary- and secondary-fluid viscosities from 1 to 10 cP and fluids with surface tensions ranging from 20 to 73 dyn/cm. However, for each jet configuration these parameters have upper limits, above which the laminar flow in the jet is disturbed by instabilities growing faster than the capillary instability leading to drop formation. Thus above these limits normal drop formation is disturbed as discussed below. These upper limits are interrelated with each other in a complicated way not yet clear from our experiments.

Finally, the primary and secondary fluids do not have to be miscible, as demonstrated in figure 6. Here a laminar-flow compound jet is generated by a primary jet consisting

of 80 % H_2O and 20 % glycerol and dye, while the secondary fluid was silicone fluid having the same viscosity as the primary fluid (Midland Silicones MS200 dimethyl silicone fluid). Now, since the surface tension of the silicone fluid to air is 20 dyn/cm and that of the water–glycerol solution 72 dyn/cm, we can deduce for the surface tension at the interfluid boundary between the primary column and the secondary fluid approximately 72–20 = 52 dyn/cm (Landau & Lifschitz 1958). Because of this large interfacial surface tension, the primary-fluid column breaks up into drops much faster than the compound jet itself, since the surface tension of the silicone-fluid/air surface is only 20 dyn/cm. Thus both primary and secondary fluids break up into drops owing to capillary instability, but at different rates and therefore at different positions (Rayleigh 1879). This explains the drop formation of the primary column within the secondary-fluid sheath of the jet. Even satellite drops of the primary fluid are generated in the silicone fluid (cf. figure 6).

4.2. *Sinuous instability*

It was mentioned earlier that the appearance of different types of instabilities depended on jet parameters. This is demonstrated in figures 7(*a–d*), where a compound jet generated by the same primary jet is shown when the secondary-fluid flow is increased. At low secondary flow the jet is stable and breaks up into droplets as shown in figure 5. An increase of the secondary flow causes the spontaneous appearance of sinuous instabilities in the jet (figure 7*b*). Further increase of secondary flow generates an extended sinuous instability (figure 7*c*). Finally, at high secondary flows, a varicose instability grows faster than the sinuous instability, thereby obscuring the latter. The series shown in figure 7 demonstrates a general fact found in all jets: independently of choice of viscosity and other properties of the primary and secondary fluid a stable jet can always be obtained if primary-jet velocity and/or secondary-fluid flow are decreased below a certain limit.

The series shown in figure 7 has been obtained by a careful choice of the primary-jet velocity and of the viscosities of the fluids used. Experiments not shown here indicate that the sinuous instability of the compound jet is initiated by a helical instability generated already inside the secondary fluid (Batchelor & Gill 1962; Reynolds 1962), which is amplified after entering the compound jet funnel. Especially at medium and large amplitudes, the effect of the ambient air tends to amplify the undulations as demonstrated in figure 7(*c*) (Weber 1931; Haenlein 1932; Phinney 1973).

It has not been possible to obtain pictures of the primary-fluid column in the sinuous compound jet as in the stable jet shown in figure 5. Therefore we do not know if the flow in the primary fluid column is still laminar. However, this is probably true, since the surface of the sinuous jet in figures 7(*b, c*) is smooth and has a constant diameter. If instabilities had occurred in the primary-fluid column, they would have caused irregularities on the compound-jet surface similar to those shown in figures 7(*d*) and 8(*a*).

4.3. *Varicose instability*

It has already been shown in figure 7(*d*) that an irregular varicose or random instability can be induced in the compound jet. The appearance of this semiturbulent instability is very similar to that observed in conventional fluid jets in air having large Reynolds numbers (> 500–3000) (Haenlein 1932; Phinney 1973; McCarthy & Molloy 1974).

Figure 8 shows two examples of this instability which seem to be caused by different types of disturbances. In figures 8(*a, b*) it is clearly seen that the primary jet is already

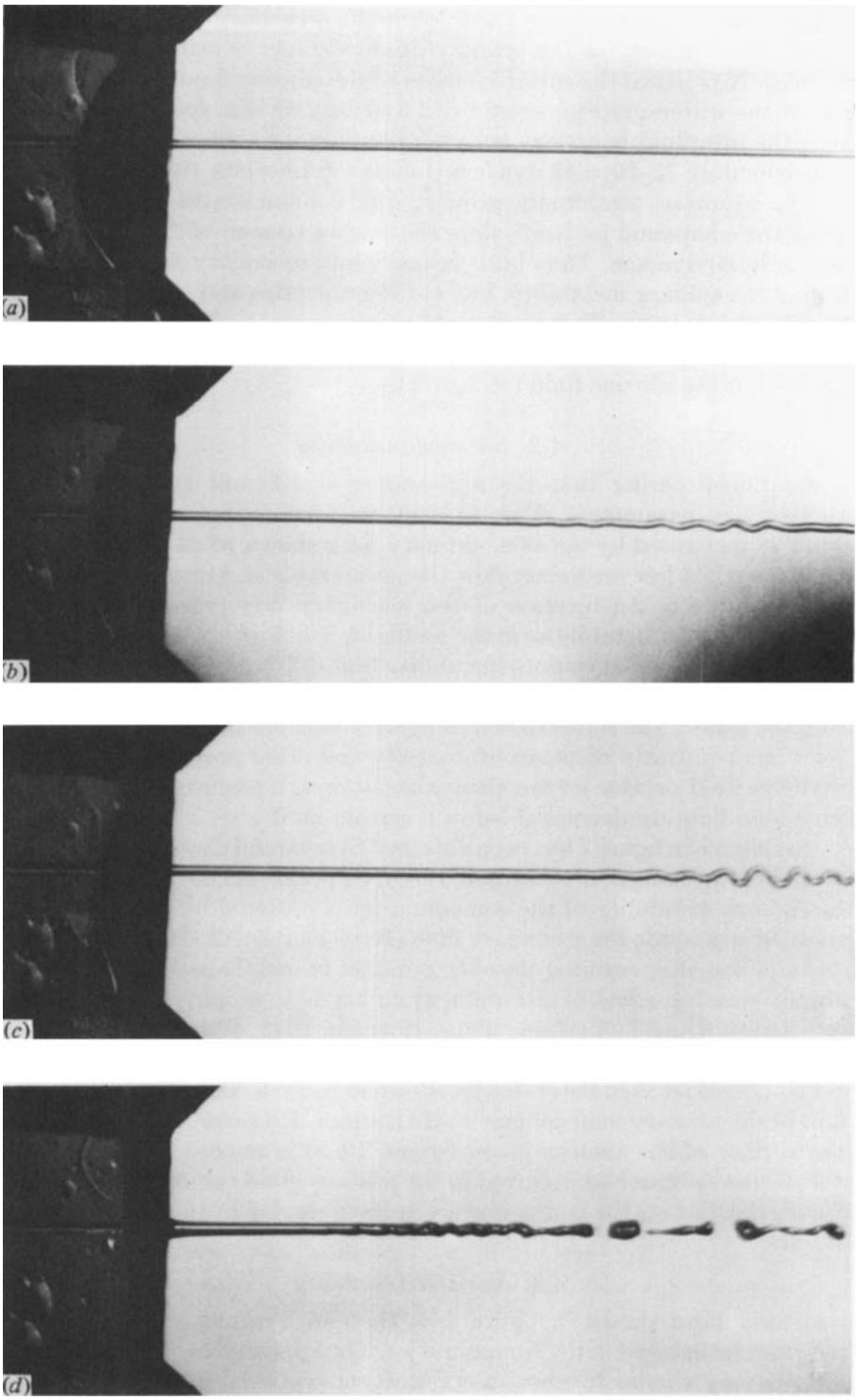

FIGURE 7. Compound jet with varying secondary-fluid flow. Primary jet H_2O, viscosity 0.95 cP. Secondary fluid 80 % H_2O + 20 % glycerol, viscosity, 1.9 cP. Primary-jet diameter 75 μm, velocity 11.1 m/s, and flow 49 μl/s are the same in all pictures. $Re_p = 876$. Secondary-fluid flow: (*a*) 5 μl/s; (*b*) 10 μl/s; (*c*) 15 μl/s; (*d*) 28 μl/s.

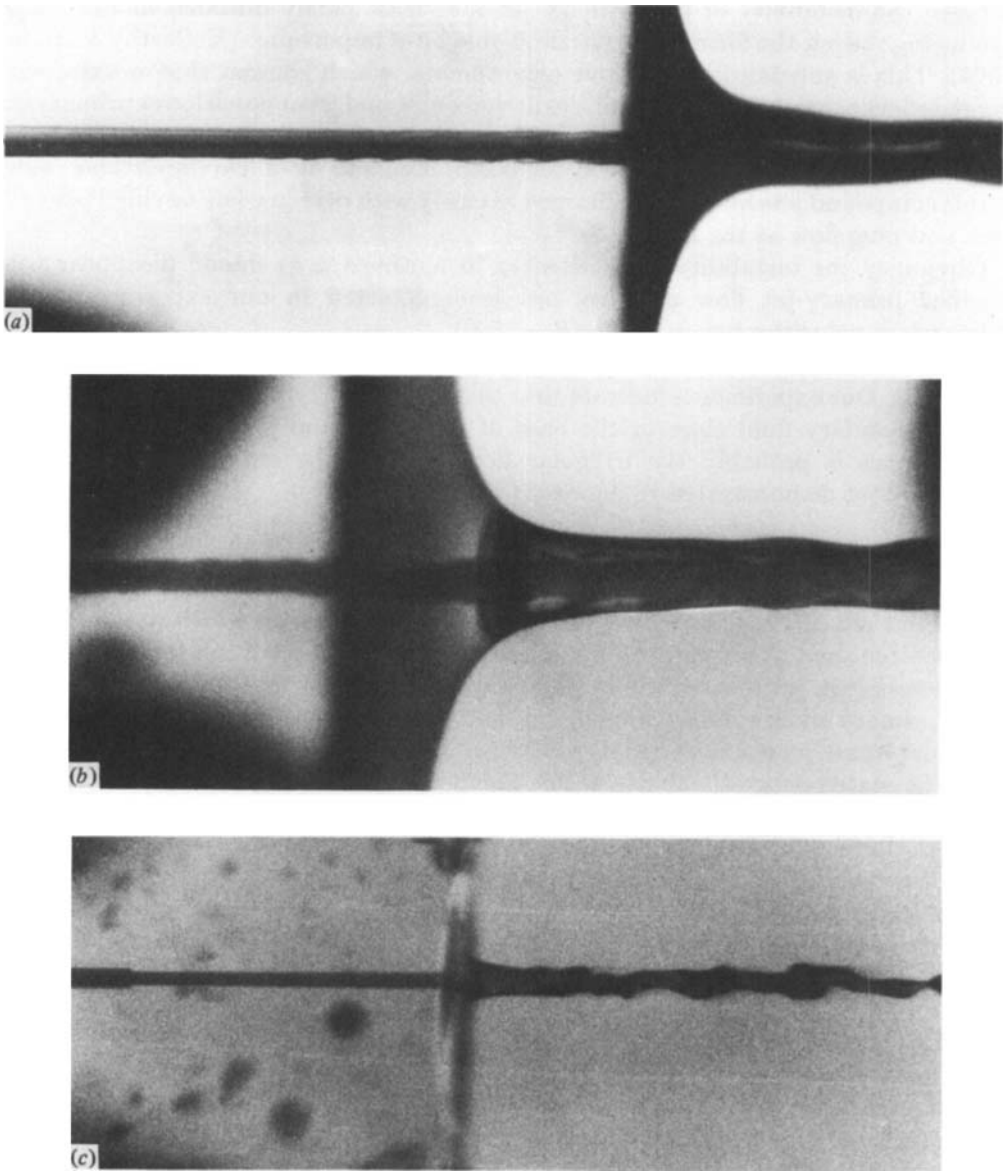

FIGURE 8. Varicose instability in compound jet. (*a*, *b*) Instability caused by semiturbulence in primary jet; primary jet 80% H_2O+20% glycerol+dye, $\bar{v}_{p0} = 8$ m/s, $Re_p = 316$; secondary fluid H_2O, $Q_s = 75$ µl/s. (*c*) Instability caused by disturbance at compound-jet base; primary jet 80% H_2O+20% glycerol+dye, $\bar{v}_{p0} = 7.5$ m/s, $Re_p = 296$; secondary fluid H_2O, flow 40 µl/s.

unstable before entering the compound-jet base. This instability is very similar to that reported by McNaughton & Sinclair (1966) for liquid-in-liquid jets with Reynolds numbers of about 1000. Since the instability is carried into the compound jet and continues to grow, it disturbs the flow in the jet and causes an irregular jet break-up into drops. As momentum is transferred more efficiently to the secondary fluid by the irregular surface of the primary jet, secondary fluid is picked up faster than in the laminar jet. At constant secondary-fluid flow this results in an appreciable shortening of the distance from the nozzle to the secondary-fluid surface.

Since the instability of the primary jet is at least partly initiated at the nozzle producing the jet, the form of the nozzle should be of importance (McCarthy & Molloy 1974). This is substantiated by our experiments, which showed that nozzles with ragged edges cause varicose instabilities in the compound jet at much lower primary-jet velocities than nozzles that were carefully ground and polished. On the other hand, the flow profile of the primary jet at the nozzle seems to be of less importance, since stable compound jets have been obtained as easily with primary jets having Poiseuille flow and plug flow at the nozzle.

Obviously the instability demonstrated in figures 8(*a*, *b*) should disappear with laminar primary-jet flow and has not been detected in our experiments with primary-jet velocities below 5 m/s ($Re < 200$).

However, even with stable primary jets, varicose instabilities have been observed (figure 8*c*). Our experiments indicate that this instability is initiated by disturbances in the secondary fluid close to the base of the compound jet. The cause of these disturbances is probably the irregular flow close to the entrance funnel to the compound jet demonstrated in figures 3(*c*, *d*).

4.4. *Conclusions*

It has been shown above that three types of instabilities can be generated in the compound jet. These instabilities are due to different causes, which are dependent on a combination of jet parameters. Since the compound jet has a large number of parameters (e.g. jet diameter, velocity, flow, viscosity, surface tension and density of the primary and secondary fluids), it has not yet been possible to understand which combinations of jet parameters give rise to the different types of instability. However, it can be stated generally that a stable compound jet develops sinuous or varicose instabilities if

(*a*) the primary jet velocity is increased;

(*b*) the ratio Q_s/Q_p of secondary to primary flow increases. Usually some kind of instability appears if $Q_s/Q_p > 4$.

(*c*) the difference between viscosities of the primary and secondary fluids is increased. Instabilities are normally encountered if they differ by a factor of more than 3 to 4.

Thus by choosing suitable parameters a stable compound jet can always be obtained which can be used for ink-jet printing.

It has also been found that small concentrations of Polyox (0.01–0.1 % in weight) in primary and/or secondary fluid effectively counteracts the instabilities described above. Since most of the instabilities observed here are initiated when the primary jet traverses the secondary fluid the reason for this should be similar to the effect of polyox on liquid-in-liquid jets described by Filipsson, Lagerstedt & Bark (1977/78).

The authors want to express their sincere gratitude to Dr Sven Bertil Nilsson for careful reading of the manuscript and helpful criticism. Thanks are also due to Professor Fritz Bark for valuable discussions.

REFERENCES

Andrade, E. N. & Tsien, L. C. 1937 *Proc. Phys. Soc. Lond.* **49**, 381.

Ashley, C. T., Edds, K. E. & Elbert, D. L. 1977 *IBM J. Res. Dev.* **21**, 69.

Batchelor, G. K. & Gill, A. E. 1962 *J. Fluid Mech.* **14**, 529.

BRUN, R. F. & LIENHARD, J. H. 1968 *ASME Paper* 68-FE-44.

CHAUDHARY, K. C. & REDEKOPP, L. G. 1980 *J. Fluid Mech.* **96**, 257.

EINSTEIN, A. 1907 *Ann. Physik* **17**, 549.

FILIPSSON, L. G. R., LAGERSTEDT, J. H. T. & BARK, F. H. 1977/78 *J. Non-Newt. Fluid Mech.* **3**, 97.

HAENLEIN, A. 1932 *NACA Tech. Memo.* 659.

HERMANRUD, B. 1981 *Dissertation Report of the Department of Electrical Measurements* LUTEDX/(TEEM-1006)/1–143.

HERMANRUD, B. & HERTZ, C. H. 1979 *J. Appl. Photogr. Engng* **5**, 220.

HERTZ, C. H. & MÅNSSON, Å. 1972 *Rev. Sci. Instrum.* **43**, 413.

HERTZBERG, L. A., SWEET, R. G. & HERTZBERG, L. A. 1976 *Sci. Am.* **234**, p. 108.

KAMPHOEFNER, F. J. 1972 *IEEE Trans. Electr. Dev.* **ED19**, 584.

LANDAU, L. D. & LIFSCHITZ, E. M. 1958 *Statistical Physics*, p. 472. Pergamon.

LANDAU, L. D. & LIFSCHITZ, E. M. 1959 *Fluid Mechanics*, p. 86. Pergamon.

LANGHAAR, H. L. 1942 *J. Appl. Mech.* **9**, A55.

LESSEN, M. & SINGH, P. J. 1973 *J. Fluid Mech.* **60**, 433.

MCCARTHY, M. J. & MOLLOY, N. A. 1974 *Chem. Engng J.* **7**, 1.

MCNAUGHTON, K. J. & SINCLAIR, C. G. 1966 *J. Fluid Mech.* **25**, 367.

PHINNEY, R. E. 1973 *J. Fluid Mech.* **60**, 689.

RAYLEIGH, LORD 1879 *Proc. Lond. Math. Soc.* **10**, 4.

REYNOLDS, A. J. 1962 *J. Fluid Mech.* **14**, 552.

SCHLICHTING, L. 1933 *Z. angew. Math. Mech.* **13**, 260.

SWEET, R. G. 1964 *Stanford Univ. Tech. Rep.* 1722–1.

TOMOTIKA, S. 1935 *Proc. R. Soc. Lond.* **A150**, 322.

WEBER, C. 1931 *Z. angew. Math. Mech.* **11**, 136.